

Correlation of Crystal Lattice Expansion and Membrane Properties for MFI Zeolites

Stephanie G. Sorenson,[†] Joseph R. Smyth,[‡] Richard D. Noble,[†] and John L. Falconer^{*†}

Department of Chemical and Biological Engineering, University of Colorado, Boulder, Colorado 80309-0424, and Department of Geological Sciences, University of Colorado, Boulder, Colorado 80309-0399

X-ray diffraction measurements show that saturation loadings of C₅–C₁₃ *n*-alkanes at room temperature increased the unit cell size of silicalite-1 crystals, and the percent volume expansion correlated linearly with the number of carbon atoms per unit cell. Adsorption of tridecane expanded the zeolite the most (1.53 vol %), but all *n*-alkanes and alcohols studied expanded MFI crystals. Pervaporation fluxes of isooctane through defects in B-ZSM-5 membranes at 313 K decreased 2 orders of magnitude when *n*-alkanes were added to the feed, and the percentage decrease correlated with crystal expansion; *n*-alkanes that expanded crystals more caused the flux through defects to decrease more.

Introduction

Studies using X-ray diffraction (XRD) have shown that zeolite crystals are flexible and deform due to changes in temperature^{1–6} and adsorption.^{7–20} The unit cell volumes of silicalite-1 and ZSM-5 crystals, both of which have MFI structures, decreased 0.47–2.2 vol % as the temperature increased over a large temperature range.^{2,3} However, the unit cell volumes increased from approximately 400 to 450 K in both studies.^{2,3} Silicalite-1 is the all-silica form of MFI zeolite, and ZSM-5 typically contains silicon, aluminum, and oxygen, although other elements beside aluminum can be incorporated into the structure. Adsorption of C₅–C₈ *n*-alkanes and isobutane were shown to expand the unit cell of silicalite-1 crystals by 0.54–1.19 vol % at room temperature, whereas benzene did not cause a significant change in the unit cell volume.⁷ Mentzen et al. reported that MFI unit cell dimensions change with *p*-xylene¹² and *n*-hexane²¹ adsorption, even at low loadings.

Defects that are larger than the zeolite pores decrease the selectivity in MFI membranes and have been imaged by confocal microscopy.^{22,23} Recent studies concluded that MFI crystal expansion caused by adsorption decreased the defect sizes in MFI membranes.^{24–28} Yu et al. found that adding low concentrations of *n*-hexane to 2,2-dimethylbutane (DMB) decreased the DMB flux by almost 2 orders of magnitude during pervaporation, so that the *n*-hexane/DMB separation selectivity was 900 times the ideal selectivity.²⁵ Because DMB is larger than MFI pores at the conditions used, it only diffused through defects. The decrease in DMB flux in the mixture was attributed to MFI crystal expansion. Thus, a membrane with significant flow through defects can separate difficult-to-separate mixtures such as organic isomers.²⁵

Permporosimetry has been used to determine the fraction of helium flow through defects.^{24,26} For a B-ZSM-5 membrane, 90% of the helium flux remained after the zeolite pores were filled with benzene, a molecule that does not expand the MFI unit cell, which means 90% of the helium flux was through defects.²⁶ However, when *n*-hexane adsorbed instead of benzene, less than 0.2% of the helium flux appeared to be through defects.²⁶ *n*-Hexane should not condense at an activity of 0.04,

and, moreover, recent studies showed that a pressure drop of 100 kPa across MFI membranes (the pressure used for the B-ZSM-5 membrane) prevents capillary condensation, even at activities of 0.9.²⁸ Thus, the decrease in helium flux was attributed to *n*-hexane-induced crystal expansion that sealed off or significantly shrank the membrane defects.²⁶ Permporosimetry measurements also demonstrated that *n*-pentane, *n*-butane, propane, ethanol, 2-propanol, 1-butanol, and SF₆ all decreased the flux through defects in MFI membranes by orders of magnitude, indicating that these molecules expanded the zeolite crystals.^{24,26,28} In contrast, the helium flux through defects *increased* when isobutane adsorbed, and this was attributed to a decrease in unit cell dimensions so that the membrane defects increased in size.²⁶

The current study is an extension of work previously published.⁷ Single-crystal XRD was used to measure the unit cell parameters of large silicalite-1 crystals with *n*-alkanes or alcohols adsorbed at room temperature. These measurements show that alcohols expand silicalite-1 crystals, and thus they could cause defect sizes to decrease in MFI membranes. *n*-Alkanes also expand silicalite-1 crystals, and the expansion correlated with reported carbon atom loading in MFI powders.²⁹ Pervaporation of isooctane was used to measure the flux through defects of two membranes at 313 K. Isooctane, which has a kinetic diameter of 0.70 nm and is thus significantly larger than MFI pores (0.55 nm), is only expected to diffuse through defects in MFI membranes. Indeed, several studies have shown that isooctane does not adsorb in MFI crystals at the experimental conditions used in this study.^{29–32} Low concentrations of *n*-alkanes were added to isooctane during pervaporation, and the isooctane flux that remained correlated with the crystal expansion; i.e., for alkanes that expanded silicalite crystals more, less isooctane diffused through the defects.

Experimental Methods

Large silicalite-1 crystals were synthesized by the method of Kornatowski³³ with crystal dimensions of L_a (length of *a*-direction) $\approx L_b \approx 45 \mu\text{m}$ and $L_c \approx 200 \mu\text{m}$,^{34,35} and uncalcined unit cell parameters of $a = 2.0058$ (1) nm, $b = 1.9924$ (1) nm, and $c = 1.3383$ (1) nm.⁷ Individual crystals were wedged into glass capillaries to secure them for XRD measurements. For measurements of the changes in crystals with adsorption, an excess of the molecule of interest was added to the capillary.⁷

* To whom correspondence should be addressed. Tel.: (303) 492-8005. E-mail: john.falconer@colorado.edu.

[†] Department of Chemical and Biological Engineering.

[‡] Department of Geological Sciences.

The capillary was placed on a goniometer, and the orientation matrix was determined using a Bruker APEX II charge-coupled device detector on a Bruker P4 diffractometer with a Mo rotating-anode X-ray source operated at 50 kV and 250 mA and an exposure time of 10 s/image. For each crystal approximately 18–24 reflections were centered in both positive and negative 2θ . The four diffractometer angles were optimized for each reflection and the unit cell parameters refined from the centered angles.

Two B-ZSM-5 membranes were synthesized by secondary growth³⁶ on the inner surface of tubular α -alumina supports (0.2 μm pores, Pall Corp.), and the preparation method was described in detail previously.³⁷ Silicalite-1 seeds were made from a gel with a molar composition of 9:24:500:96 TPAOH:SiO₂:H₂O:EtOH, where tetrapropylammonium hydroxide (TPAOH, 1.0 M aqueous solution) was used as the template and tetraethoxysilane (TEOS) was used as the silicon source. The seeds were synthesized at 358 K for 3 days. The secondary growth gel had a molar composition of 16:80:6.5:5000:320 TPAOH:SiO₂:B(OH)₃:H₂O:EtOH, corresponding to a Si/B ratio of 12.5. The gel was aged for 1 day and then was added to the inside of the seeded supports. Crystallization was carried out at 458 K for 4 h; the autoclaves were horizontal and continuously rotated. After synthesis, the membrane was washed with distilled water at room temperature to remove any remaining gel and dried at 373 K in a vacuum oven for 2 h. A second zeolite layer was grown using the same procedure. The B-ZSM-5 membranes were calcined in air at 753 K for 8 h with heating and cooling rates of 0.6 and 1.1 K/min, respectively. Scanning electron microscopy images of a B-ZSM-5 membrane synthesized by the same method showed a crystal size of $\sim 0.5 \mu\text{m}$.³⁷

Permporosity was used to measure the fraction of helium flow through defects at room temperature.^{24,26} Benzene or *n*-hexane was added to a helium stream by flowing helium through two liquid bubblers in series at 292 K, and this stream was then mixed with a second helium stream. The flow rates of the helium streams were adjusted with mass flow controllers to obtain the desired hydrocarbon activities. The hydrocarbon, which adsorbed in the MFI structure, blocked helium flow through the MFI pores at high loadings so that the remaining helium flow was through defects. The permeate pressure was approximately 84 kPa, and the pressure drop across the membrane was 96 kPa, which minimized capillary condensation.²⁸ The permeate flux of helium was measured with a bubble flow meter and a mass flow meter as a function of hydrocarbon activity. An activated carbon trap removed the hydrocarbon from the permeate stream so that only the helium flow rate was measured.

The pervaporation apparatus was described previously.³⁸ A Micropump gear pump circulated the liquid feed through the membrane at approximate 1 L/min to minimize concentration polarization. The feed reservoir contained a stir bar and was mixed throughout the experiment. Viton o-rings sealed the membrane in the stainless steel module that, along with the circulation lines, was wrapped with heating tape and insulation. A temperature controller and thermocouple kept the liquid at the desired temperature. A mechanical vacuum pump and a liquid nitrogen trap kept the permeate side pressure below 0.25 kPa. A gas chromatograph with flame ionization detector (FID) measured the feed and permeate concentration ratios.

Results and Discussion

X-ray Diffraction. X-ray diffraction measurements (Table 1) show that silicalite-1 crystals expand for saturation loadings

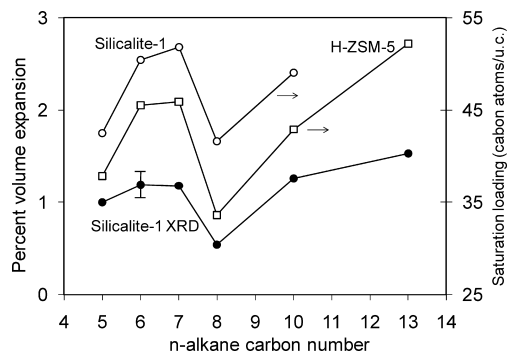


Figure 1. Percent volume expansion of the silicalite-1 unit cell at 298 K due to *n*-alkane adsorption, as measured by XRD, and the saturation loading of *n*-alkanes (carbon atoms/uc) versus the *n*-alkane carbon number. The saturation loading of *n*-alkane of silicalite-1³⁹ and H-ZSM-5²⁹ are from the literature.

Table 1. Changes in Silicalite-1 Unit Cell Parameters, As Measured by XRD, for Saturation Loadings at Room Temperature

unit cell parameter	changes in uc parameter due to adsorption of the given compound			
	decane	tridecane	ethanol	2-propanol
Δa (pm)	3.8 (6)	4.8 (9)	3.2 (9)	7.1 (9)
Δb (pm)	10.4 (5)	8.8 (9)	3.5 (9)	5.0 (9)
Δc (pm)	7.4 (6)	11.9 (9)	2.1 (9)	4.7 (8)
Δvol (nm ³)	0.0683	0.0833	0.0261	0.0518
% vol	1.26	1.53 (0.15)	0.49	0.96

of decane, tridecane, ethanol, and 2-propanol at room temperature. The unit cell (uc) volume increased from 0.49 to 1.53%. The three directions of the unit cell expanded more equally for ethanol and 2-propanol adsorption than for decane and tridecane.

The percent increase in unit cell volume is plotted in Figure 1 versus the *n*-alkane carbon number for six *n*-alkanes from C₅ to C₁₃; the C₅–C₈ values are from our previous study.⁷ Error bars on each figure are representative of the standard deviation for all of the data points. Also shown in Figure 1 are the adsorption capacities (carbon atoms/uc) reported by De Meyer et al.²⁹ for H-ZSM-5 (SiO₂/Al₂O₃ mole ratio of 80) and Sun et al.³⁹ for silicalite-1. De Meyer et al.²⁹ did simulations on silicalite-1 and liquid-phase adsorption measurements on H-ZSM-5 to obtain adsorption capacities. The simulation values were within 10% of the measured values for a given *n*-alkane. Sun et al.³⁹ obtained their adsorption capacities gravimetrically using vapor-phase adsorption. The carbon capacities measured on H-ZSM-5 and simulated on silicalite-1 at 300 K²⁹ were 5–7 carbon atoms/uc lower than the values reported by Sun et al. for silicalite-1 crystals at 303 K;³⁹ however, silicalite-1 and H-ZSM-5 show similar behavior, and their differences in loading may result because of different aluminum contents or errors in the measurements. Studies reported saturation loadings for H-ZSM-5 that differed up to 2 molecules/uc for *n*-pentane, *n*-nonane, and decane and up to 0.5 molecule/uc for *n*-hexane, *n*-heptane, and *n*-octane.^{29,39–41}

As shown in Figure 1, the percent crystal expansion has the same dependence on carbon number as the saturation loading (carbon atoms per unit cell). The drop in saturation loading for *n*-octane, relative to *n*-hexane and *n*-heptane, was attributed to the length of *n*-octane, which leads to less efficient packing within the MFI structure.²⁹ The adsorption capacities and the crystal volumes were in the following order: *n*-octane < *n*-pentane < *n*-hexane and *n*-heptane, and *n*-octane < decane < tridecane. The percent volume expansion had a linear dependence on saturation loading, as shown in Figure 2. A higher

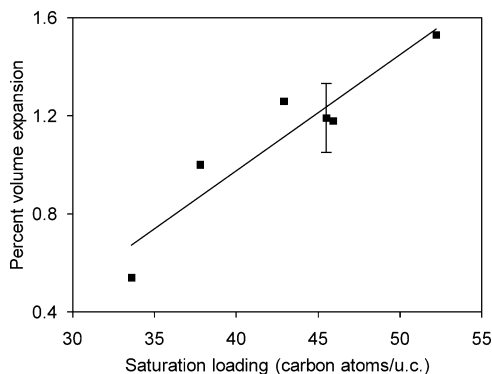


Figure 2. Percent volume expansion of the silicalite-1 unit cell at 298 K due to *n*-alkane adsorption, as measured by XRD, versus the saturation loading of *n*-alkane (carbon atoms/uc) from ref 29.

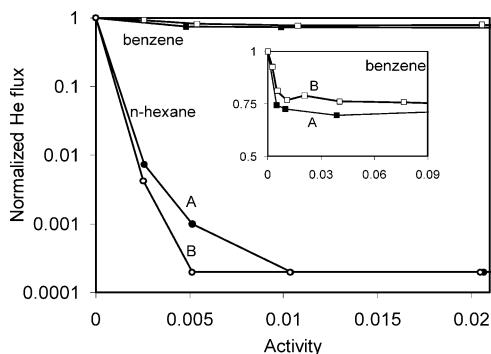


Figure 3. Normalized helium flux during pervaporation for two MFI membranes at room temperature as a function of benzene and *n*-hexane activities.

packing density of *n*-alkanes apparently created more repulsion within the MFI pores and thus expanded the crystals more.

Membrane Characterization. As shown in Figure 3, during pervaporation the helium flow through the two membranes at room temperature decreased as the benzene activity increased. For membrane A, benzene, which does not significantly expand MFI crystals, blocked 30% of the helium flow through the membrane. This means that 70% of the helium flowed through defects at room temperature. In contrast, for *n*-hexane activities above 0.01, the helium flux was below the detection limit, which means less than 0.02% of the helium flow remained. This indicates that MFI crystals expanded sufficiently when *n*-hexane adsorbed that almost all the flow through the defects was blocked. Membrane B had 75% of its helium flow through defects, based on benzene pervaporation. After *n*-hexane adsorption, the helium flux was also below the detection limit (0.02%).

Pervaporation. Pervaporation was used to characterize flow through membrane defects because the maximum flux through a membrane is obtained for a liquid feed. Because isooctane is significantly larger than the MFI pores, its diffusion is a good measure of the flux through defects.^{29,31,32,42} The isooctane flux through both membranes decreased 1–2 orders of magnitude when 0.5–6.0% *n*-alkane was added to the feed (Table 2). Xomeritakis et al. conjectured that *n*-hexane, when added to a *p*-*o*-xylene mixture, preferentially adsorbed in and blocked *o*-xylene transport through defects in MFI membranes, and thus increased *p*-*o*-xylene selectivity.⁴³ In the current study, the decreases in isooctane flux were not due to preferential adsorption in defects since *n*-alkanes and isooctane are expected to exhibit similar adsorption behavior, and the much higher isooctane concentration means that mostly isooctane adsorbed

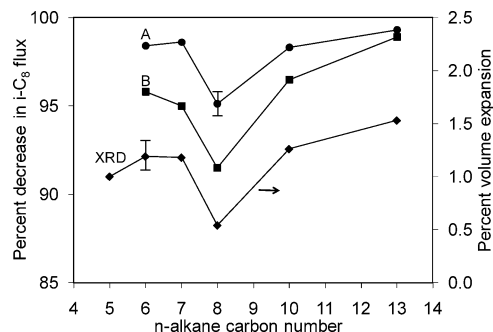


Figure 4. Percent decrease in isooctane flux, when 0.5–6.0% *n*-alkane was added to the feed, during pervaporation at 313 K for two membranes, and percent volume expansion of the silicalite-1 unit cell at 298 K due to *n*-alkane adsorption, as measured by XRD, versus the *n*-alkane carbon number.

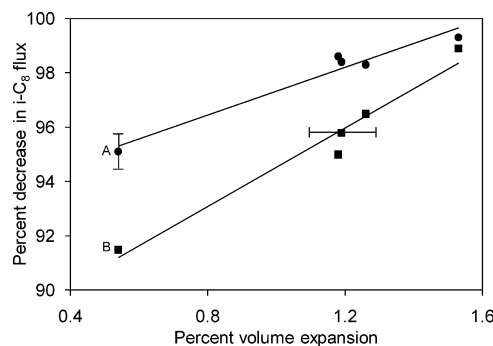


Figure 5. Percent decrease in isooctane flux, when 0.5–6.0% *n*-alkane was added to the feed, during pervaporation at 313 K for two membranes, versus the percent volume expansion of the silicalite-1 unit cell at 298 K, as measure by XRD.

Table 2. Pervaporation of Isooctane/*n*-Alkane Mixtures at 313 K

membrane			<i>n</i> -hexane	<i>n</i> -heptane	<i>n</i> -octane	decane	tridecane
A	feed wt %	100	98.6	98.7	94.0	98.4	99.4
	isooctane						
	isooctane flux (mol/m ² h)	17.9	0.29	0.25	0.88	0.30	0.13
B	feed wt %	100	99.4	97.9	99.2	98.0	99.5
	isooctane						
	isooctane flux (mol/m ² h)	14.0	0.59	0.70	1.18	0.48	0.19

in and diffused through the defects for the mixtures. Thus, the dramatic decreases in isooctane fluxes when *n*-alkanes were in the feed must be due to crystal expansion, which decreases the size of the defects.

The percentage decrease in the isooctane flux for the two membranes, after *n*-alkane addition to the feed, showed a similar dependence on the size of the *n*-alkane as the XRD volume expansion, as seen in Figure 4. Moreover, the percent decrease in isooctane flux through defects had a linear dependence on the XRD volume expansion at saturation loading, as shown in Figure 5. Of the *n*-alkanes measured, tridecane expanded the MFI crystals the most and decreased the isooctane flux the most. Only ~1% of the original isooctane flux remained for membranes A and B when tridecane adsorbed. The zeolite crystals expanded the least when *n*-octane adsorbed, and the two membranes had their highest remaining isooctane flux when *n*-octane adsorbed; 5% of the original flux remained for membrane A and 8.5% for membrane B. The defect sizes decreased in the following order: *n*-octane < *n*-hexane and *n*-heptane, and *n*-octane < decane < tridecane, which is the same order, within error ($\pm 0.7\%$), that the unit cell volume expanded.

In summary, small percentage increases in the unit cell volume of MFI crystals due to adsorption cause large decreases in fluxes through defects of MFI membranes, and when the unit cell volume increases more, the fluxes through defects decrease more.

Acknowledgment

We gratefully acknowledge support by NSF Grant CBET 0730047 and a Graduate Assistance in Areas of National Need fellowship to S.G.S. We thank Dr. Yanfeng Zhang for preparing the membranes and Drs. Milan Kocirik and Arlette Zikanova from the J. Heyrovsky Institute of Physical Chemistry Academy of Sciences of the Czech Republic for the silicalite-1 crystals. S.G.S. would like to acknowledge Dr. Gino V. Baron for his valuable discussion. X-ray diffraction was supported in part by NSF Grant EAR-0711165.

Literature Cited

- (1) Bhang, D. S.; Ramaswamy, V. High temperature thermal expansion behavior of silicalite-1 molecular sieve: In situ HTXRD study. *Microporous Mesoporous Mater.* **2007**, *103*, 235.
- (2) Marinkovic, B. A.; Jardim, P. M.; Saavedra, A.; Lau, L. Y.; Baetz, C.; de Avillez, R. R.; Rizzo, F. Negative thermal expansion in hydrated HZSM-5 orthorhombic zeolite. *Microporous Mesoporous Mater.* **2004**, *71*, 117.
- (3) Bhang, D. S.; Ramaswamy, V. Negative thermal expansion in silicalite-1 and zirconium silicalite-1 having MFI structure. *Mater. Res. Bull.* **2006**, *41*, 1392.
- (4) Marinkovic, B. A.; Jardim, P. M.; Rizzo, F.; Saavedra, A.; Lau, L. Y.; Suard, E. Complex thermal expansion properties of Al-containing HZSM-5 zeolite: A X-ray diffraction, neutron diffraction and thermogravimetry study. *Microporous Mesoporous Mater.* **2008**, *111*, 110.
- (5) Jardim, P. M.; Marinkovic, B. A.; Saavedra, A.; Lau, L. Y.; Baetz, C.; Rizzo, F. A comparison between thermal expansion properties of hydrated and dehydrated orthorhombic HZSM-5 zeolite. *Microporous Mesoporous Mater.* **2004**, *76*, 23.
- (6) Bhang, D. S.; Ramaswamy, V. Thermal stability of the Mobil Five type metallosilicate molecular sieves—An in situ high, temperature X-ray diffraction study. *Mater. Res. Bull.* **2007**, *42*, 851.
- (7) Sorenson, S. G.; Smyth, J. R.; Kocirik, M.; Zikanova, A.; Noble, R. D.; Falconer, J. L. Adsorbate-induced expansion of silicalite-1 crystals. *Ind. Eng. Chem. Res.* **2008**, *47*, 9611.
- (8) van Koningsveld, H.; Tuinstra, F.; Vanbekkum, H.; Jansen, J. C. The location of para-xylene in a single-crystal of zeolite H-ZSM-5 with a new, sorbate-induced, orthorhombic framework symmetry. *Acta Crystallogr., Sect. B: Struct. Sci.* **1989**, *45*, 423.
- (9) Lee, C. K.; Chiang, A. S. T. Adsorption of aromatic compounds in large MFI zeolite crystals. *J. Chem. Soc., Faraday Trans.* **1996**, *92*, 3445.
- (10) Bellat, J. P.; Lemaire, E.; Simon, J. M.; Weber, G.; Dubreuil, A. C. Adsorption and coadsorption of 2-methylpentane and 2,2-dimethylbutane in a ZSM-5 zeolite. *Adsorption* **2005**, *11*, 109.
- (11) Takaishi, T.; Tsutsumi, K.; Chubachi, K.; Matsumoto, A. Adsorption induced phase transition of ZSM-5 by p-xylene. *J. Chem. Soc., Faraday Trans.* **1998**, *94*, 601.
- (12) Mentzen, B. F.; Gelin, P. The silicate p-xylene system. 1. Flexibility of the MFI framework and sorption mechanism observed during p-xylene pore-filling by X-ray-powder diffraction at room-temperature. *Mater. Res. Bull.* **1995**, *30*, 373.
- (13) van Koningsveld, H.; Koegele, J. H. Preparation and structure of crystals of zeolite H-ZSM-5 loaded with p-nitroaniline. *Microporous Mater.* **1997**, *9*, 71.
- (14) Mohanty, S.; McCormick, A. V. Prospects for principles of size and shape selective separations using zeolites. *Chem. Eng. J.* **1999**, *74*, 1.
- (15) Fyfe, C. A.; Kennedy, G. J.; Deschutter, C. T.; Kokotailo, G. T. Sorbate-induced structural-changes in ZSM-5 (Silicalite). *J. Chem. Soc., Chem. Commun.* **1984**, 541.
- (16) Morell, H.; Angermund, K.; Lewis, A. R.; Brouwer, D. H.; Fyfe, C. A.; Gies, H. Structural investigation of silicalite-I loaded with n-hexane by X-ray diffraction, Si-29 MAS NMR, and molecular modeling. *Chem. Mater.* **2002**, *14*, 2192.
- (17) Mentzen, B. F.; Lefebvre, F. Flexibility of the MFI silicalite framework upon benzene adsorption at higher pore-fillings: A study by X-ray powder diffraction, NMR and molecular mechanics. *Mater. Res. Bull.* **1997**, *32*, 813.
- (18) Morell, H. Analyse der Gast-Wirt-Wechselwirkungen von n-Alkanen C₆–C₁₂ im Kanalsystem von silicalit-I. Ph.D. Thesis, Ruhr-Universität Bochum, Bochum, Germany, 2001.
- (19) Mohanty, S.; Davis, H. T.; McCormick, A. V. Sorbate/sorbent phase transition during adsorption of p-xylene in silicalite. *AIChE J.* **2000**, *46*, 1662.
- (20) Tuel, A.; Caldarelli, S.; Meden, A.; McCusker, L. B.; Baerlocher, C.; Ristic, A.; Rajic, N.; Mali, G.; Kaucic, V. NMR characterization and Rietveld refinement of the structure of rehydrated AlPO₄-34. *J. Phys. Chem. B* **2000**, *104*, 5697.
- (21) Mentzen, B. F. Energetics and siting of sorbed molecules in zeolites by computer-simulations—Comparison with calorimetric and structural results. 2. n-Alkanes in silicalite. *Mater. Res. Bull.* **1995**, *30*, 1333.
- (22) Nair, S.; Lai, Z. P.; Nikolakis, V.; Xomeritakis, G.; Bonilla, G.; Tsapatsis, M. Separation of close-boiling hydrocarbon mixtures by MFI and FAU membranes made by secondary growth. *Microporous Mesoporous Mater.* **2001**, *48*, 219.
- (23) Bonilla, G.; Tsapatsis, M.; Vlachos, D. G.; Xomeritakis, G. Fluorescence confocal optical microscopy imaging of the grain boundary structure of zeolite MFI membranes made by secondary (seeded) growth. *J. Membr. Sci.* **2001**, *182*, 103.
- (24) Yu, M.; Falconer, J. L.; Noble, R. D. Characterizing non-zeolitic pore volume in zeolite membranes by temperature-programmed desorption. *Microporous Mesoporous Mater.* **2008**, *113*, 224.
- (25) Yu, M.; Amundsen, T. J.; Hong, M.; Falconer, J. L.; Noble, R. D. Flexible nanostructure of MFI zeolite membranes. *J. Membr. Sci.* **2007**, *298*, 182.
- (26) Lee, J. B.; Funke, H.; Noble, R. D.; Falconer, J. L. High selectivities in defective MFI membranes. *J. Membr. Sci.* **2008**, *323*, 309.
- (27) Yu, M.; Falconer, J. L.; Amundsen, T. J.; Hong, M.; Noble, R. D. A controllable nanometer-sized valve. *Adv. Mater.* **2007**, *19*, 3032.
- (28) Tokay, B.; Falconer, J. L.; Noble, R. D. Alcohol and water adsorption and capillary condensation in MFI zeolite membranes. *J. Membr. Sci.* **2009**, *334*, 23.
- (29) De Meyer, K. M. A.; Chempath, S.; Denayer, J. F. M.; Martens, J. A.; Snurr, R. Q.; Baron, G. V. Packing effects in the liquid-phase adsorption of C₃–C₂₂ n-alkanes on ZSM-5. *J. Phys. Chem. B* **2003**, *107*, 10760.
- (30) Chempath, S.; Denayer, J. F. M.; De Meyer, K. M. A.; Baron, G. V.; Snurr, R. Q. Adsorption of liquid-phase alkane mixtures in silicalite: Simulations and experiment. *Langmuir* **2004**, *20*, 150.
- (31) Choudhary, V. R.; Singh, A. P. Sorption capacity and diffusion of pure liquids in ZSM-5 type zeolites. *Zeolites* **1986**, *6*, 206.
- (32) Yu, M.; Falconer, J. L.; Noble, R. D. Adsorption of liquid mixtures on silicalite-1 zeolite: A density-bottle method. *Langmuir* **2005**, *21*, 7390.
- (33) Kornatowski, J. Growth of large crystals of ZSM-5 zeolite. *Zeolites* **1988**, *8*, 77.
- (34) Kocirik, M.; Kornatowski, J.; Masarik, V.; Novak, P.; Zikanova, A.; Maixner, J. Investigation of sorption and transport of sorbate molecules in crystals of MFI structure type by iodine indicator technique. *Microporous Mesoporous Mater.* **1998**, *23*, 295.
- (35) Bräbe, L.; Kocirik, M. Silicalite-1 polycrystalline layers and crystal twins: Morphology and grain boundaries. *Mater. Chem. Phys.* **2007**, *102*, 67.
- (36) Livallo, M. C.; Tsapatsis, M. Preferentially oriented submicron silicalite membranes. *AIChE J.* **1996**, *42*, 3020.
- (37) Hong, M.; Falconer, J. L.; Noble, R. D. Modification of zeolite membranes for H₂ separation by catalytic cracking of methyldiethoxysilane. *Ind. Eng. Chem. Res.* **2005**, *44*, 4035.
- (38) Bowen, T. C.; Wyss, J. C.; Noble, R. D.; Falconer, J. L. Measurements of diffusion through a zeolite membrane using isotopic-transient pervaporation. *Microporous Mesoporous Mater.* **2004**, *71*, 199.
- (39) Sun, M. S.; Talu, O.; Shah, D. B. Adsorption equilibria of C₅–C₁₀ normal alkanes in silicalite crystals. *J. Phys. Chem.* **1996**, *100*, 17276.
- (40) Stach, H.; Lohse, U.; Thamm, H.; Schirmer, W. Adsorption equilibria of hydrocarbons on highly dealuminated zeolites. *Zeolites* **1986**, *6*, 74.
- (41) Krishna, R.; Calero, S.; Smit, B. Investigation of entropy effects during sorption of mixtures of alkanes in MFI zeolite. *Chem. Eng. J.* **2002**, *88*, 81.
- (42) Chen, N. Y.; Garwood, W. E. Some catalytic properties of ZSM-5, a new shape selective zeolite. *J. Catal.* **1978**, *52*, 453.
- (43) Xomeritakis, G.; Lai, Z. P.; Tsapatsis, M. Separation of xylene isomer vapors with oriented MFI membranes made by seeded growth. *Ind. Eng. Chem. Res.* **2001**, *40*, 544.

Received for review July 4, 2009

Revised manuscript received September 17, 2009

Accepted September 21, 2009

IE901073G